sEMG-Based Minimally Supervised Regression Using Soft-DTW Neural Networks for Robot Hand Grasping Control

Roberto Meattini, *Member, IEEE*, Alessandra Bernardini, Gianluca Palli, *Senior Member, IEEE*, and Claudio Melchiorri, *Fellow, IEEE*

***Abstract*—One of the major challenges in robotics consists in developing successful control strategies for robotic grasping devices. In this scenario, one of the most interesting approaches regards the exploitation of surface electromyography(sEMG). In this work, we propose a novel sEMG-based *minimally supervised* regression approach capable of performing nonlinear fitting without the necessity for point-by-point training data labelling. The proposed method exploits a differentiable version of the Dynamic Time Warping (DTW) similarity – referred to as soft-DTW divergence – as loss function for a flexible neural network architecture. This is a different paradigm with respect to state-of-the-art approaches in which sEMG-based control of robot hands is mainly realized using supervised or unsupervised machine learning based regression. An experimental session was carried out involving 10 healthy subjects in an offline experiment for systematic and statistical evaluations, and an online experiment for the evaluation of the control of a robot hand. The reported results demonstrate that the proposed soft-DTW neural network can be trained by means of a labelling that does not require to be temporally aligned with the sEMG training dataset, while reporting performances comparable with a standard mean square error(MSE)-based neural network. Also, the subjects were able to successfully control a robot hand for grasping motions and tasks with error levels comparable to state-of-the-art regression approaches.**

***Index Terms*—Grasping, human factors and human-in-the-loop, multifingered hands, prosthetics and exoskeletons, telerobotics and teleoperation.**

I. Introduction

HUMAN-ROBOT interfaces (HRi) for the control of robot hands are principally employed in teleoperation, prosthetics or learning by demonstration applications [1], and consist in realizing a communication channel between the operator and the robotic device based on the estimation of the operator's grasping intentions. In literature, several works have realized HRi based on forearm's muscles sEMG for the control of robot hands. Specifically, supervised machine learning based classification and regression are the two principal approaches [2]. In the classification approach, user's grasping intentions are discriminated from sEMG using a classifier that determines discrete commands for the robot hand, however presenting intrinsic reliability issues, mainly related to the unpredictability of misclassifications and complexity when the number of grasping actions increases [3]. On the other hand, regression approaches are at the base of the *simultaneous and proportional* (s/p) *control* paradigm [4], in which the operator continuously regulates grasping actions. However, also regression approaches are affected by some limitations hindering a truly intuitive and reliable sEMG-based control of robot hands. In particular, these approaches are subjected to frequent training errors, contributing in this way to the well known problem of the unreliability of sEMG-based control in real life scenarios. This is due to the fact that regression, being enforced via supervised machine learning, requires an instant by instant labelling of the sEMG training dataset. This introduces systematic labelling imprecisions, and tedious and frustrating procedures which are critical to the user [5]. To avoid this issue, several works have investigated the employment of unsupervised machine learning for s/p control of robot hands, e.g. Non-negative Matrix Factorization (NMF) [6], Principal Component Analysis (PCA) [7], and autoencoders [8]. However, the absence of labelling causes linear factorizations and autoencoders to easily fail when complex and/or multiple grasp motions are considered, due to the fact that the non-linear *fitting* capability is not available with unsupervised approaches. As a consequence, unsupervised s/p control algorithms present clear limitations in extracting meaningful commands from sEMG signals.

To overcome the limitations of state-of-the-art approaches – i.e. point-to-point labelling of the training dataset for supervised learning and unavailability of data fitting capabilities for unsupervised learning techniques – we propose an sEMG-based HRi for the control of robot hands that merges the power of non-linear fitting with the necessity of avoiding instant by instant sEMG data labelling. Specifically, we present a *minimally supervised* regression approach based on a differentiable version of the Dynamic Time Warping (DTW) similarity measure [9]. DTW is a distance-based discrepancy to evaluate similarity between

Manuscript received 24 February 2022; accepted 1 July 2022. Date of publication 22 July 2022; date of current version 2 August 2022. This letter was recommended for publication by Associate Editor D. Paez-Granados and Editor A. Peer upon evaluation of the reviewers' comments. This work was supported by the European Commission?s Horizon 2020 Framework Programme with the project REMODEL under Grant Agreement 870133. *(Corresponding author: Roberto Meattini.)*

The authors are with the Department of Electrical, Electronic, and Information Engineering, University of Bologna, 40136 Bologna, Italy (e-mail: roberto.meattini2@unibo.it; alessandr.bernardin5@unibo.it; gianluca.palli@unibo.it; claudio.melchiorri@unibo.it).

This letter has supplementary downloadable material available at https://doi.org/10.1109/LRA.2022.3193247, provided by the authors.

Digital Object Identifier 10.1109/LRA.2022.3193247

temporal sequences in a more general manner with respect to classical static Euclidean distance based measures. Indeed, DTW is invariant to phase misalignments, speed and sampling rate differences, and non-linear temporal distortions [10]. DTW has been used in previous studies for the classification of sEMG [11], vision [12] and Inertial Measurement Units (IMUs) [13] data. It has been also exploited for the evaluation of sEMG-based s/p control performance [7], and for the averaging of time series [14]. We exploit the properties of DTW to realize a neural network architecture that can be trained through a labelling that is independent from the actual temporal execution of the grasping motions during the sEMG training dataset acquisition. From a computational point of view, the described approach requires to use the DTW as a fitting loss function, which is not possible since the DTW is not differentiable. We therefore use a smoothed version, named *soft-DTW divergence* [15], which is differentiable, non-negative and minimized for identical temporal sequences, and can therefore be used as fitting term for a minimally supervised regression via a flexible neural network architecture. In this study, a soft-DTW Neural Network (soft-DTW NN) for minimally supervised regression of forearm sEMG signals is proposed and tested for robot hand grasping control. The aim is to show that this sEMG-based HRi allows to perform s/p control avoiding instant by instant labelling of sEMG training data, while, at the same time, exploiting the advantage of non-linear fitting provided by the neural network architecture. Experiments were carried out engaging a group of 10 subjects. Specifically, we report for the outcome of both offline experiments (involving five of the subjects) for a systematic evaluation and statistical analysis of the soft-DTW NN performance, and online experiments (involving the other five subjects) in which s/p control of both a simulated and real robot hand was assessed for repeated grasping and motion control tasks.

II. Materials and Methods

In this section we present a NN architecture to perform nonlinear regression of sEMG signals into control commands, avoiding instant-by-instant labelling of the training dataset. Specifically, we present the NN structure, along with the soft-DTW based loss function used to train the network in a minimally supervised way. Since control commands are extracted from myoelectric signals, we first describe the experimental setup used for sEMG signals acquisition and processing. Those commands are then exploited to control the UBHand robot hand. We therefore present the control law used to regulate power, tripodal and ulnar grasping motions.

A. Experimental Setup

1) Wearable sEMG Sensing and Signal Processing: The sEMG signals were acquired from the operator's forearm muscles, by means of the 8-channels wearable sEMG armband gForcePro, by OYMotion[1] (Fig. 1). Specifically, the armband was placed in proximity of the *Flexor Digitorum Superficialis* and *Extensor Digitorum Communis* bellies muscles, referring to procedures and best practices outlined in [16]. The raw sEMG signals were acquired at 1 kHz from the armband by means of an embedded Bluetooth interface, and streamed to a nearby PC. Then, a processing chain was applied to each sEMG channel, composed by the following filtering operations [17]: *(i)* a 50 Hz notch filter for powerline interference cancellation, *(ii)* a 20 Hz highpass filter for baseline noise reduction, and *(iii)* the computation of the root mean square (RMS) value of the signal over a 200 ms running window.

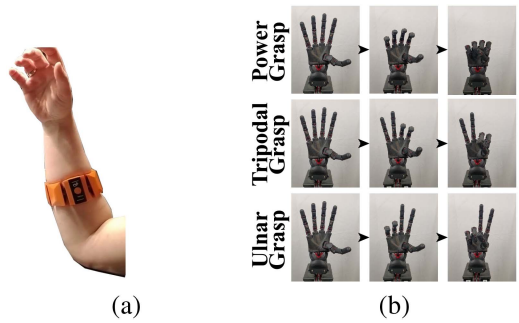

Fig. 1. (a) gForcePro sEMG armband worn on the forearm. (b) UB Hand robot hand.

2) Robot Hand Description and Controller: The grasping device used to test the proposed minimally supervised sEMG regression is the UB Hand IV [18] (in the following simply UBHand), a dexterous anthropomorphic robot hand (Fig. 1). In particular, two versions were used, the real UBHand and its simulator. The real UBHand is a five-fingered fully-actuated anthropomorphic robot hand [18], with 15 DoF driven by 25 tendons, each of the latter actuated by a servomotor. In this study, the robot hand controller was implemented in order to allow the regulation of three different motions corresponding to the power, tripodal and ulnar grasps (Fig. 1). In detail, considering that the hand presents $n_J = 15$ joints (3 joints for each finger) actuated by $n_T = 25$ tendons, the vector of UBHand joint reference angles $\theta_J^{\text{ref}}(t)$ is imposed as

$$\theta_J^{\text{ref}}(t) = S\alpha(t), \tag{1}$$

where $S \in \mathbb{R}^{n_J \times 3}$ is the grasp synergy matrix containing, in its first, second and third column, the joint weights that allow to regulate the closure of the power, tripodal and ulnar grasps, respectively, by modulating the synergistic reference $\alpha(t) = [\alpha_{\text{PO}}(t)\ \alpha_{\text{TR}}(t)\ \alpha_{\text{UL}}(t)]^T \in \mathbb{R}^3$ between the range of values [0,1]. In particular, the weights of S are computed in such a way that the hand poses match the maximum closure level of power, tripodal and ulnar grasp for $\alpha_{PO}(t) = 1, \alpha_{TR}(t) = 1$ and $\alpha_{UL}(t) = 1$, respectively. At the lower level the robot hand servomotors, thanks to their embedded electronics, are controlled according to

$$\tau(t) = K(\theta_M^{\text{ref}}(t) - \theta_M(t)), \tag{2}$$

where $\tau(t) \in \mathbb{R}^{n_T}$ denotes the vector of servomotor torques, K is a proper diagonal matrix determining the motor stiffnesses, $\theta_M(t) \in \mathbb{R}^{n_T}$ the current servomotor angles, and $\theta_M^{\text{ref}}(t) =$

[1][Online]. Available: http://www.oymotion.com/

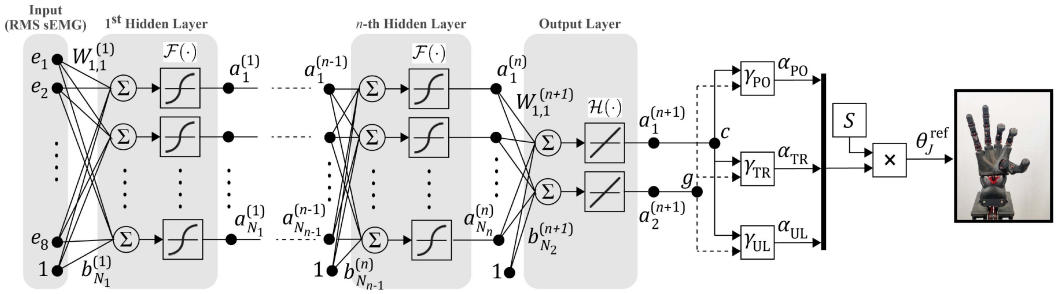

Fig. 2. Soft-DTW Neural Network architecture and grasp control scheme.

$H\theta_J^{\text{ref}}(t)$ is the reference servomotor angles, being $H \in \mathbb{R}^{n_T \times n_J}$ a map between motor and joint spaces as defined in our previous works, for more details see [18], [19]. Therefore, by modulating the components of $\alpha(t)$ in (1) it was possible to regulate power, tripodal and ulnar grasps singularly and with smooth transitions from one grasp to another.

B. Soft-DTW Neural Network

1) Network Architecture and Grasp Control: A feed-forward neural network was used in conjunction with a soft-DTW based loss function in order to perform a minimally supervised regression of sEMG signals, that is a regression in which an instant by instant labelling of the training dataset was not required. Let us consider the vector of RMS sEMG signals (see Section II-A1), denoted as $E(t) = [e_1(t)\, e_2(t) \cdots e_8(t)]^T$, which was applied to the input of the soft-DTW NN as shown in Fig. 2. According to the figure, let us consider the network structure as composed by n hidden layers and an output layer. The generic j–th hidden layer contains N_j neurons with hyperbolic tangent sigmoid transfer function $\mathcal{F}(\cdot)$ and bias vector $b^{(j)} \in \mathbb{R}^{N_j}$, with the input vector $a^{(j-1)}(t) \in \mathbb{R}^{N_{j-1}}$ (coinciding with the output of the $(j-1)$–th hidden layer with N_{j-1} neurons, except for the first hidden layer in which the input is $E(t)$) passing through the weight matrix $W^{(j)} \in \mathbb{R}^{N_j \times N_{j-1}}$. According to this notation, the output vector of the j–th hidden layer $a^{(j)}(t) \in \mathbb{R}^{N_j}$ is given by

$$a^{(j)}(t) = \mathcal{F}(W^{(j)} a^{(j-1)}(t) + b^{(j)}). \tag{3}$$

The output layer – the $(n+1)$–th layer of the network – contains two neurons (i.e. $N_{n+1} = 2$) with linear transfer function $\mathcal{H}(\cdot)$ and, therefore, the output vector of the network $a^{(n+1)}(t) \in \mathbb{R}^{N_{n+1}}$ is described by

$$a^{(n+1)}(t) = \begin{bmatrix} a_1^{(n+1)}(t) \\ a_2^{(n+1)}(t) \end{bmatrix} = \mathcal{H}(W^{(n+1)} a^{(n)}(t) + b^{(n+1)}), \tag{4}$$

where $a_1^{(n+1)}(t)$ and $a_2^{(n+1)}(t)$ are the two scalar outputs of the network, and $a^{(n)}(t) \in \mathbb{R}^{N_n}$, $W^{(n+1)} \in \mathbb{R}^{N_{n+1} \times N_n}$ and $b^{(n+1)} \in \mathbb{R}^{N_{n+1}}$ are the input vector, weight matrix and bias vector of the output layer.

The goal of the introduced network was to perform a minimally supervised nonlinear regression of sEMG signals into control signals. Therefore, the network had to be trained in order to select its parameters – i.e. the weight matrices and bias vectors of (3) and (4) – such that the two outputs $a_1^{(n+1)}(t)$ and $a_2^{(n+1)}(t)$ in (4) allow to control the robot hand grasp closure level and type, respectively. Specifically, defining

$$c(t) := a_1^{(n+1)}(t) \quad \text{and} \quad g(t) := a_2^{(n+1)}(t), \tag{5}$$

for the robot hand control we impose

$$\begin{aligned} \alpha_{\text{PO}}(t) &= \gamma_{\text{PO}}\, c(t), \\ \alpha_{\text{TR}}(t) &= \gamma_{\text{TR}}\, c(t), \\ \alpha_{\text{UL}}(t) &= \gamma_{\text{UL}}\, c(t), \end{aligned} \tag{6}$$

where $\alpha_{\text{PO}}(t)$, $\alpha_{\text{TR}}(t)$ and $\alpha_{\text{UL}}(t)$ are the synergistic references for the power, tripodal and ulnar grasps, respectively, previously introduced in (1), and

$$\gamma_{\text{PO}} = \gamma_{\text{PO}}(g(t)) = \begin{cases} \frac{g(t)}{g_1^-}, & \text{if } 0 \le g(t) \le g_1^- \\ 1, & \text{if } g_1^- < g(t) < g_1^+ \\ \frac{g(t)-g_2^-}{g_1^+-g_2^-} & \text{if } g_1^+ \le g(t) \le g_2^- \\ 0, & \text{otherwise} \end{cases}, \tag{7}$$

$$\gamma_{\text{TR}} = \gamma_{\text{TR}}(g(t)) = \begin{cases} \frac{g(t)-g_1^+}{g_2^--g_1^+}, & \text{if } g_1^+ \le g(t) \le g_2^- \\ 1, & \text{if } g_2^- < g(t) < g_2^+ \\ \frac{g(t)-g_3^-}{g_2^+-g_3^-} & \text{if } g_2^+ \le g(t) \le g_3^- \\ 0, & \text{otherwise} \end{cases}, \tag{8}$$

$$\gamma_{\text{UL}} = \gamma_{\text{UL}}(g(t)) = \begin{cases} \frac{g(t)-g_2^+}{g_3^--g_2^+}, & \text{if } g_2^+ \le g(t) \le g_3^- \\ 1, & \text{if } g_3^- < g(t) < g_3^+ \\ \frac{g(t)-g_4}{g_3^+-g_4} & \text{if } g_3^+ \le g(t) \le g_4 \\ 0, & \text{otherwise} \end{cases}, \tag{9}$$

are gains with a trapezoidal profile (see Fig. 3), in which $g_i^+ = g_i + \delta$, $g_i^- = g_i - \delta$ $(i = \{1, 2, 3\})$ and we set $g_1 = 1$, $g_2 = 2$, $g_3 = 3$, $g_4 = 4$ and $\delta = 0.3$. In this way, $c(t)$ in (6) has the task to regulating the closure level of the power, tripodal and ulnar grasps, based on the value of the gains γ_{PO}, γ_{TR} and γ_{UL} according to (7)–(9) (see Fig. 3), the latter allowing a continuous transition among the different grasps.

2) Loss Function and Minimally Supervised Training: The network training was performed with the scaled conjugate gradient back-propagation algorithm [20]. According to the concept and notations introduced in the previous subsection, the loss function used was the soft-DTW divergence [15] between the

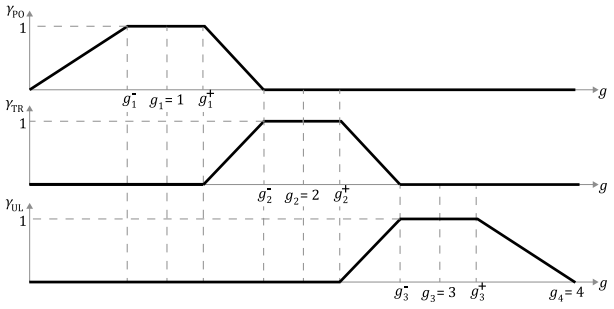

Fig. 3. Profile of the gains γ_{PO}, γ_{TR} and γ_{UL}, described by (7)–(9).

network 2-dimensional output $A_T \in \mathbb{R}^{2\times d}$, obtained by applying at the network inputs a 8-dimensional sEMG training dataset $E_T \in \mathbb{R}^{8\times d}$ (see Section II-A1), and the 2-dimensional target output $T \in \mathbb{R}^{2\times d}$ with a length of d samples. Specifically, the soft-DTW divergence loss function is given [15] by

$$D(A_T, T) = S(A_T, T) - \frac{1}{2}S(A_T, A_T) - \frac{1}{2}S(T, T), \quad (10)$$

where $S(A_T, T)$ is the soft-DTW operator [21]

$$S(A_T, T) = \min_{\pi\in\mathcal{A}(A_T,T)}^{\lambda} \sum_{i,j\in\pi} d(a_{T_i}, t_j)^2, \quad (11)$$

where $a_{T_i}, t_j \in \mathbb{R}^2$ indicates 2-dimensional elements of A_T, T, respectively, $d(a_{T_i}, t_j)^2$ denotes the squared Euclidean distance operator, and $\min^{\lambda}$ is the *soft-min* operator defined [21], considering a generic function $f(x)$, as

$$\min_x^{\lambda} f(x) = -\lambda \log \sum_x \exp\left(\frac{-f(x)}{\lambda}\right), \quad (12)$$

in which $\lambda > 0$ is a parameter such that, for $\lambda \to 0^+$, the soft-DTW $S(\cdot,\cdot)$ coincides with the standard non-differentiable DTW. In this work, we set $\lambda = 0.1$. Finally, in (11), $\mathcal{A}(A_T, T)$ denotes the set of all admissible alignment paths [22] between A_T and T. We recall that, denoting by x and y two generic time series of respective lengths n and m, a path $\pi \in \mathcal{A}(x, y)$ of length K is a sequence $(\pi_0, \ldots, \pi_k, \ldots, \pi_{K-1})$, which elements are index pairs $\pi_k = (i_k, j_k)$ such that

i) $0 \le i_k < n, 0 \le j_k < m$;
ii) $\pi_0 = (0, 0), \pi_{K-1} = (n-1, m-1)$;
iii) $\forall\, k > 0$, considering $\pi_k = (i_k, j_k)$ and $\pi_{k-1} = (i_{k-1}, j_{k-1})$, it holds:

- $i_{k-1} \le i_k \le i_{k-1} + 1$;
- $j_{k-1} \le j_k \le j_{k-1} + 1$.

For the sake of clarity, Fig. 4 reports exemplifying alignment paths. Please refer to [15], [22] for further details. The soft-DTW divergence based loss function introduced in (10) can be explicitly differentiated and, therefore, used within the back-propagation algorithm in order to train the neural network. The gradient of (10) was obtained as

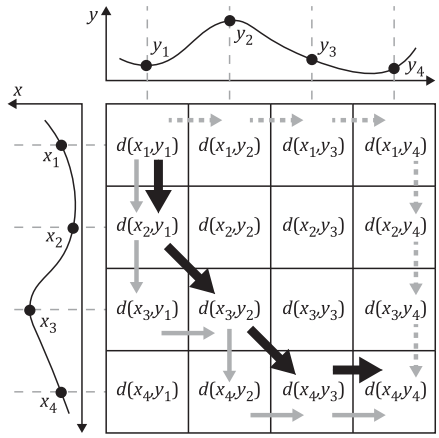

Fig. 4. Exemplifying alignment paths between generic signals x and y of four samples. The black arrows denote the DTW alignment path, whereas the solid and dashed gray arrows indicates other generic alignment paths.

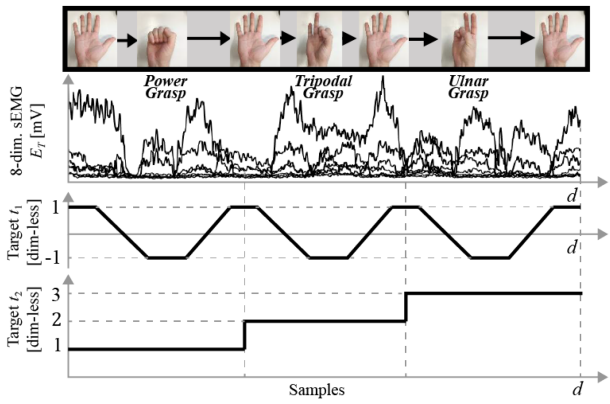

Fig. 5. Target outputs t_1 and t_2 (middle and bottom graphs), defined on the basis of the length of d samples of the sEMG training dataset (top graph). Note that the sEMG training dataset was recorded without any reference to follow nor synchronization with the target output (which was defined *a posteriori*). Accordingly hand gestures at the top of the figure are not alligned with targets $t1$ and $t2$.

$$\nabla_{A_T} D(A_T, T) = \left(\frac{\partial \Delta(A_T, T)}{\partial A_T}\right) \Pi_{(A_T,T)} + - \frac{1}{2}\left(\frac{\partial \Delta(A_T, A_T)}{\partial A_T}\right) \Pi_{(A_T,A_T)} \quad (13)$$

where $\Delta(A_T, T)$ is the matrix that stores the squared Euclidean distances $d(a_{T_i}, t_j)^2$, $\partial\Delta(A_T, T)/\partial A_T$ is the Jacobian of $\Delta(A_T, T)$ with respect to A_T, $\Pi_{(A_T,T)}$ and $\Pi_{(A_T,A_T)}$ are the soft-DTW alignment path matrices between (A_T, T) and (A_T, A_T), respectively (we refer the reader to [21] for details on alignment path matrices and soft-DTW alignment path matrix). The target output T is given once the sEMG training dataset E_T is provided. Specifically, looking at Fig. 5, the user is required to execute the following sequence of continuous grasping motions, starting from the hand completely open, while the sEMG data is acquired and stored in $E_T \in \mathbb{R}^{8\times d}$: *(i)* power grasp closure followed by power grasp opening; *(ii)* tripodal grasp closure followed by tripodal grasp opening; *(iii)* ulnar grasp closure

followed by ulnar grasp opening (see Fig. 5). The execution of this sequence of grasping motions does not require the user to follow any reference artificial hand. Then, the target output $T = [t_1\ t_2]^T \in \mathbb{R}^{2\times d}$ is defined as described in the following. t_1 presents a trapezoidal profile between -1 and 1, uniformly distributed along the d samples given by the sEMG training set, resembling the three closure levels of the power, tripodal and ulnar grasps according to (1), and t_2 indicates the grasp related to each of the three closure levels (see Fig. 5), where the values 1, 2 and 3 indicate the power, tripodal and ulnar grasps, respectively, in accordance with (7)–(9). Note that no instant-by-instant labelling is required.

III. Experiments and Results

A. Subjects

We engaged 10 healthy subjects (1 female, age: 25, and 9 males, age: 30.5 ± 4 ? right handed: 9 sbjs., left handed: 1 sbj). In the following, the subjects will be referred as S1, S2,..., S10. Five of the subjects (S1,..., S5) were involved in an offline experimental session, where sEMG signals were recorded for a systematic evaluation of the proposed soft-DTW NN compared with the performance of a standard (mean square error)MSE-based NN (see Section III-C). The other five subjects (S6,..., S10) were involved in an online experimental session (see Section III-D), and were required to online control both a simulated robot hand (see Section III-D1) in order to replicate reference continuous grasping motions, and a real robot hand (see Section III-D3) to perform the grasping of different objects. The experiment was conducted in accordance with the Declaration of Helsinki and all participants were thoroughly informed about the experimental protocol and asked to sign an informed consent form.

B. Experimental Recordings

During experiments, the subjects were seated in front of a table and their forearm sEMG signals were recorded in accordance to Section II-A1. For the offline dataset acquisition, the five subjects were asked to execute six times the sequence of power, tripodal and ulnar grasps, as depicted in Fig. 5. Importantly, for the only purpose of the offline study, the subjects were instructed to follow the motions of a reference graphical simulator of the UBHand robot hand shown on a screen. The reference simulated hand was made to move very slowly (1 minute and 30 seconds for each sequence of power, tripodal and ulnar grasp motions), for attempting to minimize as much as possible the desynchronization between simulated and subject?s hand motions. Differently, for online training dataset acquisition, the participants were instructed to perform only two repetitions of the sequence of power, tripodal and ulnar grasps, without any visual reference. Note that the reduced number of repetitions was intended to highlight the potentialities of our NN, which can be used even with a relatively small amount of data. Once the acquisition was completed, the sEMG signals were stored as a dataset to be used for NN training.

C. Offline Experimental Session

The subjects involved in the offline experiment were asked to execute a sequence of gestures as described in Section III-B, and the related recorded myoelectric signals were exploited to train the network and then to evaluate the performance of the proposed soft-DTW NN using the ANOVA test, as reported in details in the following of this section.

1) Offline Motion With Desynchronization Task: In the offline experiment, we were interested in systematically evaluating the capability of the proposed soft-DTW NN to tolerate inaccurate point-by-point labelling of sEMG signals. Therefore, we want to study the effect of having the target output T (previously introduced in Section II-B2) not synchronized with the grasping motions performed by the subjects during the sEMG training dataset acquisition. In this scenario, the performance obtained with the soft-DTW NN were also compared with the performance of a standard MSE-based NN, i.e. a NN trained in the same labelling circumstances but using the standard MSE as loss function. To this aim, the subjects were asked to execute for six times continuous closing/opening motions of the power, tripodal and ulnar grasps in sequence, while following a reference simulated hand, as explained in Section III-B. We then used the simulated hand motion reference to build three different types of target outputs for the training of the NN: *(i)* the *synchronized target*, which was directly obtained from the motion of the simulated hand (i.e. corresponding to an sEMG signal labelling *almost*-synchronized with the subject's hand motion); *(ii)* the *target shrunk by 1/3*, which was obtained by shrinking the synchronized target by one-third of its length, keeping the same initial point and holding the last value until matching the length of the original non-shrunk target (i.e. corresponding to a labelling slightly desynchronized with the subject's hand motion); and, finally, *(iii)* the *target shrunk by 2/3*, obtained in a manner analogous to the target shrunk by 1/3, but shrunk by two-thirds of the original target length (i.e. corresponding to a labelling highly desynchronized with the subject's hand motion). Then, six different nested cross-validations (CV) were applied to the sEMG dataset recorded from each of the subjects involved in the offline experimental session (composed by 6 repetitions of the sequence of power, tripodal and ulnar grasp closing/opening motions), one for each combination of NN (soft-DTW and MSE-based) and target output (synchronized, shrunk by 1/3 and shrunk by 2/3). In detail, each nested CV was composed by two nested loops. The inner loop consisted in a 5-fold CV, in which a grid-search was conducted for the selection of the best combination of number of NN hidden layers and neurons per hidden layer (see Section II-B1). The outer loop consisted in a 6-fold CV for the evaluation of the performance of the NN architecture that won in the inner loop, tested on a separated external fold. The final result of the CV was then computed by averaging the six NN performance values obtained from the outer loop. Note that each fold corresponded to a single sequence of power, tripodal and ulnar grasp closing/opening motions. The metric used to compute the NN performance values in the CV nested loops was the standard DTW, because it represents a particularly appropriate distance measure for offline evaluations

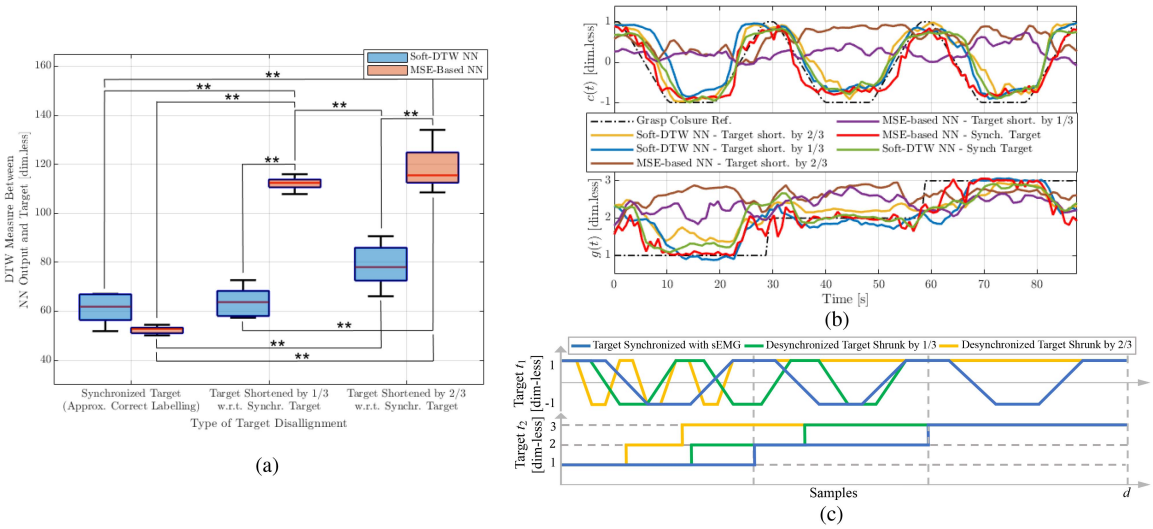

Fig. 6. Results of the offline experimental session. (a) Boxplot of the aggregated results, over the subjects, of the nested CV (see Section III-C). The symbol "$**$" indicates a statistically significant difference ($p < .01$), whereas the absence of the symbol indicates no statistically significant difference. (b) Example of the NN outputs for the different combinations of NN and target types, reported from a single validation fold of the outer loop of the nested CV for the subject S1. (c) Target outputs used to train the NN: synchronized target, target shrunk by 1/3 and target shrunk by 2/3.

of sEMG-based s/p control approaches [7]. A Matlab code version of the described nested CV and related soft-DTW NN implementation has been released in GitHub at the repository.[2]

2) Results of the Offline Motion With Desynchronization Task: The results of the offline experimental session can be observed in the boxplots reported in Fig. 6(a), grouped based on the different target outputs used for the NN training within the CV, for the soft-DTW and MSE-based NN types. On these results, a two-way repeated measures Analysis of Variance (ANOVA) was conducted. The two investigated factors were *NN type* (soft-DTW, MSE-based) and *target output type* (synchronized, shrunk by 1/3, shrunk by 2/3), and the statistical significance was set to $p < .05$. The Shapiro-Wilk test for normality check was performed, reporting that the assumption of normality was not violated. The Mauchly's test was performed to check the assumption of sphericity, indicating a violation for both the main and interaction effects, $W = 3.75 \cdot 10^{-18}$, $p < .001$. Consequently, the respective Greenhouse-Geisser estimate of sphericity correction was applied. The result of the two-way ANOVA revealed a statistically significant interaction between the factors NN type and target output type, $F(0.66, 2.64) = 19.24$, $p < 0.05$. Therefore, as usual in these cases, we analyzed the data reported in Fig. 6(a) as separate groups in a one-factor design, and performed a one-way ANOVA, which revealed the presence of a statistically significant difference, $F(1.56, 6.6) = 27.85$, $p < .01$. Therefore, following the one-way ANOVA, we finally performed a Games-Howell test (appropriate in presence of sphericity assumption violations) for pairwise comparison of the different groups of data in Fig. 6(a). According to the symbols "$**$" in Fig. 6(a) indicating the groups of data statistically significantly different, it results from the pairwise comparison that no statistically significant difference was present between the performance obtained by the proposed soft-DTW NN trained with the synchronized, shrunk by 1/3 or shrunk by 2/3 target, and the MSE-based NN trained with the synchronized target. This demonstrates the robustness of the proposed sEMG-based minimally supervised regression approach to both slightly and highly desynchronizations between sEMG signals and related labelling. Fig. 6(b) shows, as an example, the outputs of the offline experiment for a single validation fold of the CV outer loop for the subject S1, where it is possible to observe that all the soft-DTW NN and MSE-based NN trained on the synchronized target were able to approximately follow the reference, whereas critically degraded performance were shown by the MSE-based NN trained with the target shrunk by 1/3 and 2/3.

[2][Online]. Available: https://github.com/TipeaTapei/sDTW-Neural-Network

D. Online Experimental Session

The subjects involved in the online experiment were required to online control both the simulated and real UBHand robot hand using the proposed sEMG-based minimally supervised regression approach as illustrated in Sections II-A2 and II-B1. In particular, for each subject, the soft-DTW NN were trained according to Sections II-B2 and III-B.

1) Motion Following Task: In the first task of the online experimental session, each subject was asked to control the simulated UBHand. In particular, two simulated robot hands were shown on a screen, and the subject was required to control only one of the two, in order to instantaneously replicate reference power, tripodal and ulnar grasping motions shown by the other simulated hand (see Fig. 7), i.e. carrying out a motion following task.

2) Results of the Motion Following Task: Fig. 7(a) reports the online controlled grasp closure level $c(t)$ and grasp type $g(t)$ (according to notation of (5)) averaged over the subjects involved in the online experimental session. It can be observed that, on

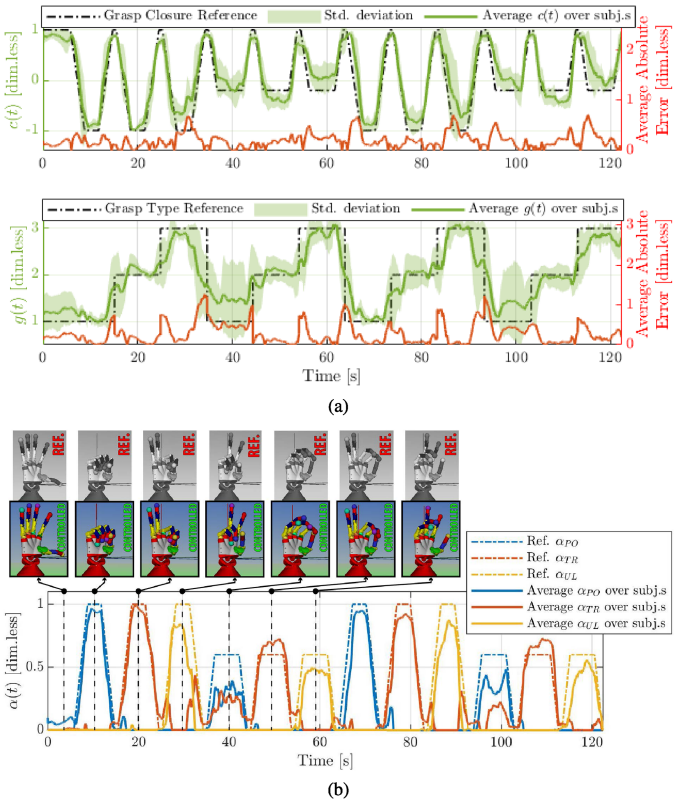

Fig. 7. Results of the online experimental session for the motion following task, controlling the simulated UBHand. (a) Average controlled grasp closure level $c(t)$ and grasp type $g(t)$ (see (5)), over the subjects involved in the online experiment, along with standard deviation and average absolute error with respect to the motion of a reference hand that was required to be followed. (b) Average synergistic reference signals $\alpha(t)$ (see (1)) and some related configuration of the controlled and reference simulated robot hands.

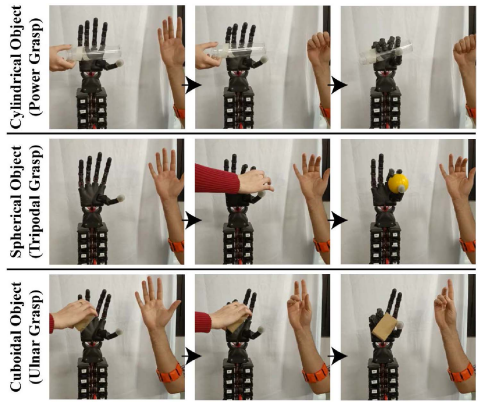

Fig. 8. Frames from the video recording of the online experiment during the object grasping task with real UBHand, for the subject S6.

average, the subjects followed continuous reference grasping motions with acceptable accuracy, reporting for a maximum average absolute error equal to 0.62 for the grasp closure and 1.28 for the grasp type (see Fig. 7(a)). In this relation, in order to provide a better positioning of the obtained error levels with respect to previous works on regression of sEMG signals into hand kinematics, we also report that the results in Fig. 7(a) correspond —on average over the subjects— to an R^2 value, a normalized MSE (nMSE) and a root-MSE (RMSE) equal to: *(i)* 0.7878, 0.2122 and 0.133, respectively, for the grasp closure; and *(ii)* 0.7294, 0.2706 and 0.3088, respectively, for the grasp type. For the comparison, we report the results obtained by three important/pioneering works related to sEMG signal regression: *(i)* in [23] an R^2 value in the range 0.8–0.9 was reported using Kernel Ridge Regression (KRR); *(ii)* in [24] a nMSE in the range 0.2–0.3 was reported when using Kernel Ridge Regression (KRR); and (*iii*) in [25] (refer also to [26]) a RMSE in the range 0.07–0.08 was reported using Long Short-Term Memory (LSTM) NN. Therefore, even if these previous studies were characterized by different experiments and protocols, it is possible to appreciate that the results obtained with the proposed soft-DTW NN achieved a close error to the ones obtained by the selected previous works, the latter based on supervised approaches. In this relation, the meaning of using the soft-DTW NN approach with respect to state-of-the-art supervised regression techniques lies in the fact of obtaining comparable performances with considerable less effort for the training recording session, since no instrumentation/specific procedures are required to enforce temporal synchronization between training data and labels. This, along with the fact that the soft-DTW approach has the capability of compensating for the systematic labels-trainset synchronization imprecisions of supervised approaches, paves the way to a novel minimally supervised regression paradigm that can significantly contribute in reducing the reliability issue shown by sEMG-based control in real life applications outside of laboratory settings.

Furthermore, Fig. 7(b) reports the average temporal evolution, over the subjects, of the synergistic references $\alpha_{PO}(t)$, $\alpha_{TR}(t)$ and $\alpha_{UL}(t)$ (see (1)) corresponding to the actual average control inputs of the simulated UBHand, obtained by applying (6) to the signals of Fig. 7(a). In Fig. 7(b), it is worth highlighting how a correct control of the power grasp motion could be obtained by a proper combination of α_{PO} and α_{TR}, without necessarily matching the related reference signals (dotted lines in Fig. 7(b)) obtained by applying (6) to the reference signals of Fig. 7(a). This justifies the higher absolute error for the grasp type in Fig. 7(a) around the time instants 40 s and 100 s, which, in reality, did not produce incorrect online motion tracking performance (see the frames of the reference and controlled simulated UBHand in Fig. 7(b)).

3) Object Grasping Task: In the second and last online experiment task, the subjects were required to control the real UBHand in order to perform object grasping. Specifically, each subject had to grasp three different types of objects: a cylinder, a sphere and a cuboid using the power, tripodal and ulnar grasp, respectively (see Fig. 8).

4) Results of the Object Grasping Task: We report that all the subjects involved in the online experimental session successfully performed a stable grasp of the three objects, confirming, also for the control of a real robot hand, the positive control performance already registered with the results obtained in the offline experiment and in the online control of the simulated robot hand. Fig. 8 reports the frames of a video recording of the online object grasping task carried out by the subject S6,

showing the successful grasping of the cylindrical, spherical and cuboidal objects by continuously controlling power, tripodal and ulnar grasps on the real UBHand.

IV. Conclusion

In this article, a soft-DTW NN for sEMG-based minimally supervised regression for s/p control of robot hands has been presented. The proposed approach has been illustrated, and the result of an experimental evaluation involving 10 healthy subjects–five in an offline experiment and five in an online experiment– has been reported. In the offline experimental session, the robustness of the proposed soft-DTW NN to temporal misalignment between the NN target output and the sEMG training dataset has been demonstrated, also supported by statistical evidence. In the online experimental session, the involved subjects were able to successfully continuously control the grasping motions of a simulated robot hand, and to perform the grasping of different objects controlling power, tripodal and ulnar grasps on a real robot hand. The advancements offered for control purposes by the proposed method are related to the fact that complex training procedures can be avoided. Indeed, labels-trainset synchronization procedures, which are necessary in state-of-the-art supervised regression approaches, introduce complications related to the tiring/frustration of the users and to the fact that a perfectly synchronized labelling of physiological data is not possible in practice even with very complex instrumentation and procedures. This makes, *de facto*, the training procedure of supervised approaches difficult to be correctly performed in real scenarios, therefore playing a role in the very well known problem of degradation of performances and unreliability of sEMG-based control of robot hands. The proposed soft-DTW NN goes in the direction of the possibility of improving control performance by avoiding complex training procedures, as it is also attempted by state-of-the-art unsupervised regression approaches, but with the additional capability of nonlinear fitting by means of a minimally-supervised approach. Future investigations will regard the improvement of the NN architecture for enhanced computational efficiency, improved convergence of the NN training algorithm and better performance. We will also consider the usage of deep learning architectures for the increase of the set of grasp types controllable on the robot hand.

References

[1] C. Melchiorri, *Robot Teleoperation*. London, U.K.: Springer, 2013, pp. 1–14.

[2] A. Ameri, E. N. Kamavuako, E. J. Scheme, K. B. Englehart, and P. A. Parker, "Support vector regression for improved real-time, simultaneous myoelectric control," *IEEE Trans. Neural Syst. Rehabil. Eng.*, vol. 22, no. 6, pp. 1198–1209, Nov. 2014.

[3] K. A. Ingraham, L. H. Smith, A. M. Simon, and L. J. Hargrove, "Nonlinear mappings between discrete and simultaneous motions to decrease training burden of simultaneous pattern recognition myoelectric control," in *Proc. IEEE 37th Annu. Int. Conf. Eng. Med. Biol. Soc.*, 2015, pp. 1675–1678.

[4] R. Meattini, M. Nowak, C. Melchiorri, and C. Castellini, "Automated instability detection for interactive myocontrol of prosthetic hands," *Front. Neurorobot.*, vol. 13, 2019, Art. no. 68.

[5] H. Hermens, S. Stramigioli, H. Rietman, P. Veltink, and S. Misra, "Myoelectric forearm prostheses: State of the art from a user-centered perspective," *J. Rehabil. Res. Dev.*, vol. 48, no. 6, 2011, Art. no. 719.

[6] C. Lin, B. Wang, N. Jiang, and D. Farina, "Robust extraction of basis functions for simultaneous and proportional myoelectric control via sparse non-negative matrix factorization," *J. Neural Eng.*, vol. 15, no. 2, 2018, Art. no. 026017.

[7] R. Meattini, D. De Gregorio, G. Palli, and C. Melchiorri, "Design and evaluation of a factorization-based grasp myoelectric control founded on synergies," in *Proc. IEEE 12th Int. Workshop Robot Motion Control*, 2019, pp. 252–257.

[8] I. Vujaklija, V. Shalchyan, E. N. Kamavuako, N. Jiang, H. R. Marateb, and D. Farina, "Online mapping of EMG signals into kinematics by autoencoding," *J. Neuroeng. Rehabil.*, vol. 15, no. 1, pp. 1–9, 2018.

[9] M. Müller, "Dynamic time warping," in *Information Retrieval for Music and Motion*. Berlin, Germany: Springer, 2007, pp. 69–84.

[10] E. J. Keogh and M. J. Pazzani, "Scaling up dynamic time warping for datamining applications," in *Proc. 6th ACM SIGKDD Int. Conf. Knowl. Discov. Data Mining*, 2000, pp. 285–289.

[11] M. Atzori, H. Müller, and M. Baechler, "Recognition of hand movements in a trans-radial amputated subject by sEMG," in *Proc. IEEE 13th Int. Conf. Rehabil. Robot.*, 2013, pp. 1–5.

[12] M. AbdelMaseeh, T.-W. Chen, and D. W. Stashuk, "Extraction and classification of multichannel electromyographic activation trajectories for hand movement recognition," *IEEE Trans. Neural Syst. Rehabil. Eng.*, vol. 24, no. 6, pp. 662–673, Jun. 2016.

[13] A. Akl and S. Valaee, "Accelerometer-based gesture recognition via dynamic-time warping, affinity propagation, & compressive sensing," in *Proc. IEEE Int. Conf. Acoust., Speech Signal Process.*, 2010, pp. 2270–2273.

[14] D. Schultz and B. Jain, "Nonsmooth analysis and subgradient methods for averaging in dynamic time warping spaces," *Pattern Recognit.*, vol. 74, pp. 340–358, 2018.

[15] M. Blondel, A. Mensch, and J.-P. Vert, "Differentiable divergences between time series," in *Proc. Int. Conf. Artif. Intell. Statist.*, 2021, pp. 3853–3861.

[16] A. O. Perotto, *Anatomical Guide for the Electromyographer: The Limbs and Trunk*. Springfield, IL, USA: Charles C. Thomas Publisher, 2011.

[17] R. Meattini, S. Benatti, U. Scarcia, D. De Gregorio, L. Benini, and C. Melchiorri, "An sEMG-based human-robot interface for robotic hands using machine learning and synergies," *IEEE Trans. Compon. Packag. Manuf. Technol.*, vol. 8, no. 7, pp. 1149–1158, Jul. 2018.

[18] C. Melchiorri, G. Palli, G. Berselli, and G. Vassura, "Development of the UB hand IV: Overview of design solutions and enabling technologies," *IEEE Robot. Automat. Mag.*, vol. 20, no. 3, pp. 72–81, Sep. 2013.

[19] G. Palli et al., "The dexmart hand: Mechatronic design and experimental evaluation of synergy-based control for human-like grasping," *Int. J. Robot. Res.*, vol. 33, no. 5, pp. 799–824, 2014.

[20] M. F. Møller, "A scaled conjugate gradient algorithm for fast supervised learning," *Neural Netw.*, vol. 6, no. 4, pp. 525–533, 1993.

[21] M. Cuturi and M. Blondel, "Soft-DTW: A differentiable loss function for time-series," in *Proc. Int. Conf. Mach. Learn.*, 2017, pp. 894–903.

[22] H. Sakoe and S. Chiba, "Dynamic programming algorithm optimization for spoken word recognition," *IEEE Trans. Acoust., Speech, Signal Process.*, vol. 26, no. 1, pp. 43–49, Feb. 1978.

[23] J. M. Hahne et al., "Linear and nonlinear regression techniques for simultaneous and proportional myoelectric control," *IEEE Trans. Neural Syst. Rehabil. Eng.*, vol. 22, no. 2, pp. 269–279, Mar. 2014.

[24] A. Gijsberts et al., "Stable myoelectric control of a hand prosthesis using non-linear incremental learning," *Front. Neurorobot.*, vol. 8, 2014, Art. no. 8.

[25] A. E. Olsson, N. Malešević, A. Björkman, and C. Antfolk, "End-to-end estimation of hand-and wrist forces from raw intramuscular EMG signals using LSTM networks," *Front. Neurosci.*, vol. 15, 2021, Art. no. 777329.

[26] A. H. Al-Timemy, C. Castellini, J. Escudero, R. Khushaba, and S. Muceli, "Current trends in deep learning for movement analysis and prosthesis control," *Front. Neurosci.*, vol. 16, 2022, Art. no. 889202.